Article

Current Biology

fMRI Reveals a Novel Region for Evaluating Acoustic Information for Mate Choice in a Female Songbird

Highlights

- fMRI reveals two courtship song-selective forebrain regions in female finches
- Responses of an integrative region (NCC) parallel behavioral preferences
- Auditory area CMM may be sensitive to acoustic differences in tempo
- The NCC may be a novel node for evaluating acoustic courtship signals

Authors

Lisbeth Van Ruijssevelt, Yining Chen, Kaya von Eugen, ..., Onur Güntürkün, Sarah C. Woolley, Annemie Van der Linden

Correspondence

sarah.woolley@mcgill.ca (S.C.W.), annemie.vanderlinden@uantwerpen.be (A.V.d.L.)

In Brief

Using fMRI, Van Ruijssevelt et al. uncover an integrative sensory region (NCC) that responds selectively to courtship songs in female zebra finches. Moreover, unlike auditory regions, activity in the NCC parallels behavioral preferences and thus appears to be a novel node in the avian circuitry for evaluating acoustic information for mate choice.

Van Ruijssevelt et al., 2018, Current Biology *28*, 1–11
March 5, 2018
https://doi.org/10.1016/j.cub.2018.01.048

CellPress

Please cite this article in press as: Van Ruijssevelt et al., fMRI Reveals a Novel Region for Evaluating Acoustic Information for Mate Choice in a Female Songbird, Current Biology (2018), https://doi.org/10.1016/j.cub.2018.01.048

Current Biology
Article

fMRI Reveals a Novel Region for Evaluating Acoustic Information for Mate Choice in a Female Songbird

Lisbeth Van Ruijssevelt,[1] Yining Chen,[2] Kaya von Eugen,[3] Julie Hamaide,[1] Geert De Groof,[1] Marleen Verhoye,[1] Onur Güntürkün,[3] Sarah C. Woolley,[2,4,*] and Annemie Van der Linden[1,4,5,*]
[1]Bio-Imaging lab, Department of Biomedical Sciences, University of Antwerp, 2610 Antwerpen, Belgium
[2]Department of Biology, McGill University, Montreal QC H3A 1B1, Canada
[3]AE Biopsychologie, Fakultät für Psychologie, Ruhr-Universität Bochum, 44801 Bochum, Germany
[4]These authors contributed equally
[5]Lead Contact
*Correspondence: sarah.woolley@mcgill.ca (S.C.W.), annemie.vanderlinden@uantwerpen.be (A.V.d.L.)
https://doi.org/10.1016/j.cub.2018.01.048

SUMMARY

Selection of sexual partners is among the most critical decisions that individuals make and is therefore strongly shaped by evolution. In social species, where communication signals can convey substantial information about the identity, state, or quality of the signaler, accurate interpretation of communication signals for mate choice is crucial. Despite the importance of social information processing, to date, relatively little is known about the neurobiological mechanisms that contribute to sexual decision making and preferences. In this study, we used a combination of whole-brain functional magnetic resonance imaging (fMRI), immediate early gene expression, and behavior tests to identify the circuits that are important for the perception and evaluation of courtship songs in a female songbird, the zebra finch (*Taeniopygia guttata*). Female zebra finches are sensitive to subtle differences in male song performance and strongly prefer the longer, faster, and more stereotyped courtship songs to non-courtship renditions. Using BOLD fMRI and EGR1 expression assays, we uncovered a novel region involved in auditory perceptual decision making located in a sensory integrative region of the avian central nidopallium outside the traditionally studied auditory forebrain pathways. Changes in activity in this region in response to acoustically similar but categorically divergent stimuli showed stronger parallels to behavioral responses than an auditory sensory region. These data highlight a potential role for the caudocentral nidopallium (NCC) as a novel node in the avian circuitry underlying the evaluation of acoustic signals and their use in mate choice.

INTRODUCTION

Sexual selection potently shapes both the production and perception of courtship signals across species [1–3]. In order to be effective, courtship signals must be accurately detected and perceived, and consequently, the sensory and even cognitive systems of receivers critically influence the evolution of signal production in response to sexual selection by mate choice [2, 3]. For example, in Túngara frogs, the spectral properties of advertisement calls match the tuning properties of the peripheral auditory end organs of receivers, indicating that the properties of receiver's auditory systems may have shaped the evolution of advertisement calls [4]. At the same time, female Túngara frog cognitive discrimination abilities have been proposed to constrain call elaboration and complexity [5]. In songbirds, female birds can exert acute influences on the learning and production of song by males. For example, female cowbirds use rapid motor displays to indicate to juvenile males which elements to retain in their song repertoire [6]. Thus, the sensory and cognitive biases of female receivers can shape signal production even in the context of a culturally transmitted trait. Despite the importance of female perceptual and cognitive systems for mate choice and signal evolution, there is a surprising lack of knowledge on the neural mechanisms that contribute to sexual decision making and preferences.

Songbirds are a classic model for studying the neural basis of vocal communication. In many species, males produce a complex, learned vocalization, the song, which conveys substantial information about the identity, state, and quality of the signaler [7], and both song learning and production depend on specialized neural circuitry known as the "song system" [8, 9]. Song is a key trait used in mate-choice decisions, and female receivers must thus accurately assess and interpret the information song provides. In zebra finches, females show preferences for the songs of different males, as well as for songs performed in different social contexts [10–13]. For example, females prefer the longer, faster, and more stereotyped courtship song ("female-directed" or FD song) over songs performed when a

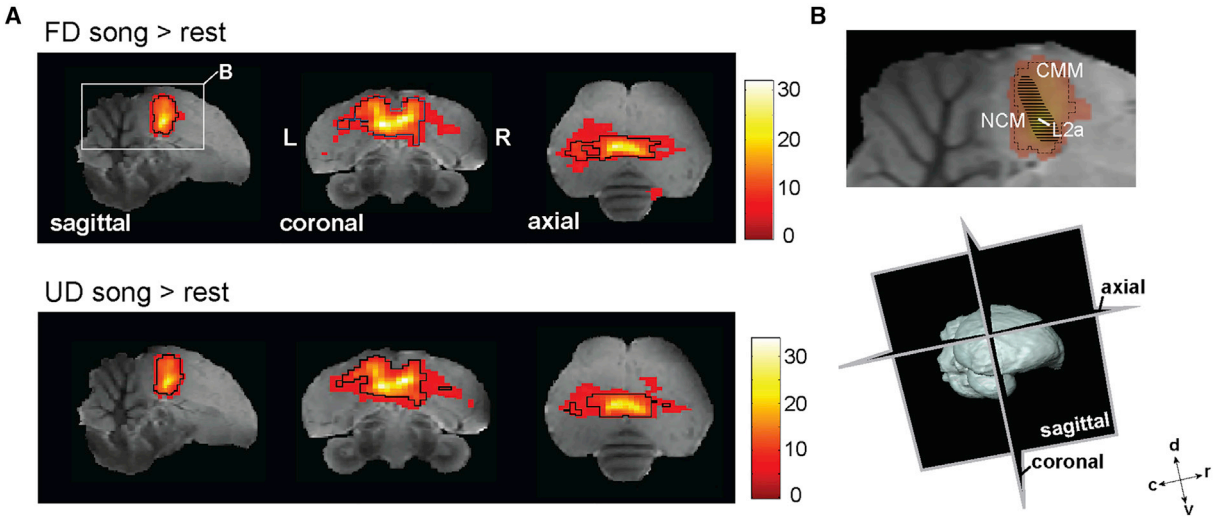

Figure 1. Song Playback Induces Robust Responses throughout the Auditory Forebrain

(A) Auditory forebrain activation in response to FD (top) and UD (bottom) songs. Statistical group maps are superimposed on images from the zebra finch MRI atlas [22]. Voxel t values are color coded according to the scales on the right, and only voxels with t values > 4.79 ($p < 0.0001$) are displayed. The black contours delineate voxels with t values > 7.47 ($p_{FWE}<0.05$).

(B) Inset from the sagittal view in (A) indicating the location of the primary auditory subfield L2a as well as the secondary auditory regions CMM and NCM.

Abbreviations: (FD) female directed; (UD) undirected; (CMM) caudomedial mesopallium; (NCM) caudomedial nidopallium; (c) caudal; (d) dorsal; (L) left; (R) right; (r) rostral; (v) ventral. (n = 17).

See also Figure S1.

male is alone ("undirected" or UD song) even when the song is from an unfamiliar singer [13, 14]. However, while female song preferences have been the focus of considerable study, little is known about the specific neural circuits in females, especially circuits beyond the canonical auditory system, that are necessary for the perception of, preference for, and response to courtship signals.

One challenge in the study of neural processes of song preference is that most methods commonly used in songbird research require the *a priori* selection of particular region(s) of interest (ROIs) and often involve comparison between individuals that have heard different stimuli. While this approach works well on identified circuits like the classical auditory pathway, it has limited ability to uncover novel ROIs. In contrast, functional magnetic resonance imaging (fMRI) can infer neural activity at the level of the whole brain and differential neural responses to a range of different stimuli can be investigated within a single individual. Therefore, we used blood-oxygen level dependent (BOLD) fMRI—which has previously been successfully implemented in songbirds [15–18] —to elucidate the neural substrates of the processing of FD songs at the level of the whole brain in female zebra finches. Our fMRI data, validated by immunocytochemistry (ICC), identified two regions selectively activated by FD versus UD songs. The pattern of activity in one of these regions, the caudocentral nidopallium (NCC), paralleled the behavioral responses of females. In contrast, activity in an auditory sensory region, the caudomedial mesopallium (CMM), was similar in response to songs with shared temporal acoustic patterns. Thus, to our knowledge, these are the first data to identify a potential role of the NCC as a novel node in the avian circuitry underlying the evaluation of acoustic signals and their use in mate choice.

RESULTS

fMRI Reveals Two Forebrain Regions with Greater Activation in Response to FD Song

Previous investigation of the neural circuits that are important for song perception and preference have focused on a limited subset of mainly auditory regions in the songbird caudal forebrain. To search more broadly for regions differentially affected by variation in the acoustic features of song driven by changes in social context, we used fMRI to assess neural activity across forebrain regions in adult female zebra finches in response to unfamiliar FD and UD song stimuli. In line with previous studies (e.g., [19–21]), song playback elicited robust auditory responses, evidenced by reproducible BOLD signals, in the auditory forebrain (analogous to the mammalian auditory cortex), including the primary auditory area Field L and (parts of) the secondary auditory areas caudomedial mesopallium (CMM) and caudomedial nidopallium (NCM) (Figure 1 and Figure S1A).

However, while auditory responses were widespread, only a limited subset of forebrain regions responded differentially to the social-context-dependent variation in the acoustic features of the stimulus. Specifically, voxel-based analysis of the data revealed two clusters of voxels, one in the auditory CMM and one in a multisensory integrative forebrain area the caudocentral nidopallium (NCC), which both exhibited a higher BOLD response to FD songs versus UD songs (paired t test). In the auditory forebrain, we found a cluster of 10 significant voxels in the CMM (T_{max} = 4.3621, p_{uncorr} = 0.0002; Figures 2A–2D; one voxel = 0.125 × 0.125 × 0.400 mm^3), lateralized to the right hemisphere. We also discovered a second significant cluster of 37 significant voxels, lateralized to the left hemisphere, within a

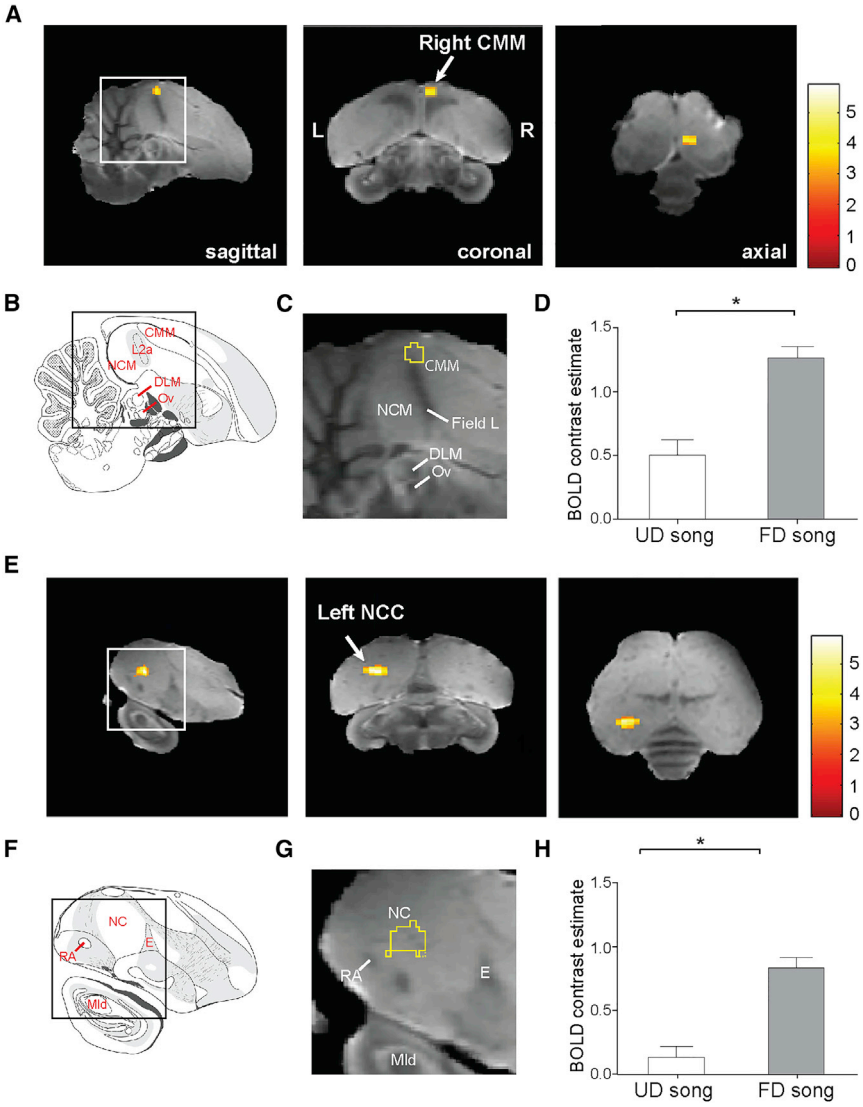

Figure 2. fMRI Reveals Two Regions that Are Selective for FD Songs

Significantly higher BOLD responses induced by FD song playback compared to UD song playback were identified in the caudomedial mesopallium (CMM; A–D) and the caudocentral nidopallium (NCC; E–H).

(A and E) Three views (sagittal [left], coronal [middle], and axial [right]) of the respective clusters in the CMM (A) and the NCC (B) with significantly higher BOLD responses induced by FD song playback relative to UD song playback. Images are statistical maps superimposed on zebra finch MRI atlas images [22]. t values are color coded according to the scale (right), and all cluster voxels with t values > 2.60 ($p < 0.01$) are displayed. The coronal (middle) panel highlights the substantial lateralization of the BOLD response.

(B and F) Line drawings of sagittal sections from the zebra finch histological atlas browser (Oregon Health & Science University, Portland, OR 97239; http://www.zebrafinchatlas.org [23]).

(C and G) Detailed view of the exact locations of the clusters within the CMM and the NCC (magnification of the region outlined in black in, respectively, [B] and [F]).

(D and H) The relative BOLD response amplitude (versus rest) in the identified cluster was significantly greater in response to FD than UD songs. The values (± SEM) are from the voxel with the maximum t value (FD versus UD), and the zero level corresponds to the estimated mean during rest periods.

Abbreviations: (FD) female directed; (UD) undirected; (CMM) caudomedial mesopallium; (DLM) medial dorsolateral nucleus of the anterior thalamus; (E) entopallium; (Mld) dorsal part of the later mesencephalic nucleus; (NCM) caudomedial nidopallium; (NCC) caudocentral nidopallium; (Ov) nucleus ovoidalis; (RA) robust nucleus of the arcopallium. (*$p_{uncorr} < 0.001$; n = 17).

See also Figure S1.

portion of the multisensory integrative forebrain region the NCC ($T_{max} = 5.8893$, $p_{uncorr}<0.0001$; Figures 2E–2H). Here, we only detected positive BOLD responses (versus rest; $p_{uncorr}<0.001$) to FD songs, but not to UD songs. Thus, the voxel-based analysis identified two regions with selectivity for FD songs and, in both regions, the FD selectivity was exclusively in one hemisphere.

Given the striking laterality of the selectivity for FD songs (e.g., Figures 2A and 2E), we further investigated the hemispheric difference using an ROI approach (see STAR Methods). For this, we compared the average BOLD responses to FD and UD songs directly between the FD-song-selective clusters in the dominant hemisphere versus their counterparts in the opposite hemisphere. We found a significant interaction of stimulus and hemisphere in both the CMM ($F_{(1,16)} = 7.8557$, $p = 0.0128$) and the NCC ($F_{(1,16)} = 10.7059$, $p = 0.0048$) (Figure 3). Similar to the voxel-based analysis, this interaction indicates that FD songs induce significantly higher responses than UD songs in the right CMM only ($p < 0.0001$). In contrast, for the NCC, only the left hemisphere demonstrated significantly higher responses for FD versus UD songs ($p < 0.0001$). In addition, the response to FD songs in the NCC was higher in the left hemisphere than the right hemisphere ($p = 0.0170$). Further, to confirm FD selectivity and response lateralization in these areas, we also applied the ROI approach to responses to pure tone stimuli in CMM and NCC. Responses to the pure tone stimuli were significantly lower than the responses to FD songs in both regions (Figure S1B and S1C; CMM $p = 0.0114$; NCC $p = 0.0035$) and were similar to responses to UD songs (CMM $p = 0.7657$; NCC $p = 0.6227$). Moreover, there was no apparent lateralization of the responses to pure tones in either the CMM ($F_{(1,16)} = 1.4537$, $p = 0.2455$) or the NCC ($F_{(1,16)} = 2.3910$, $p = 0.1416$; Figures S1D and S1E). Thus, the ROI-based analysis confirmed the FD song selectivity in CMM and NCC and the specific lateralization of these FD-song-selective responses as determined earlier in the voxel-based analysis.

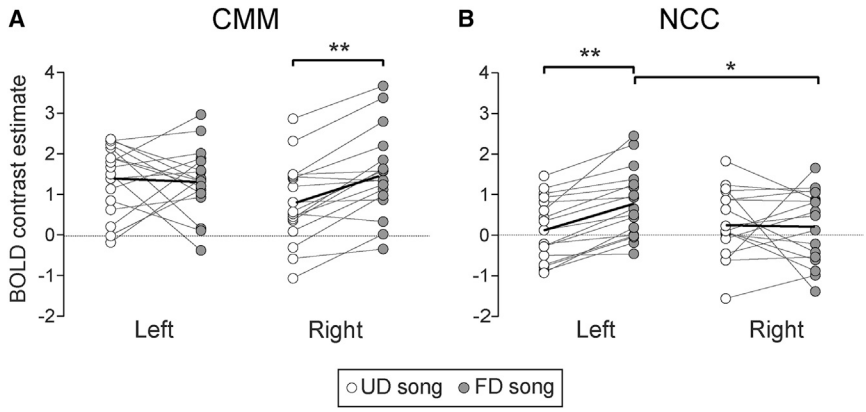

Figure 3. BOLD Response to FD and UD Song in Female Zebra Finches Is Highly Lateralized

(A and B) Average relative BOLD response amplitude (versus rest) in the CMM (A) and the NCC (B) elicited by FD and UD songs across voxels within the identified FD-song-selective clusters (right CMM and left NCC) and their mirrored counterparts. The zero level corresponds to the estimated mean during rest periods. The bold line corresponds to the group mean, and points are responses for individual females.

Abbreviations: (FD) female directed; (UD) undirected; (CMM) caudomedial mesopallium; (NCC) caudocentral nidopallium. (*$p < 0.05$; **$p < 0.001$; $n = 17$).

See also Figure S1.

EGR1 Expression Patterns in the CMM and the NCC Support fMRI Results

The finding that the CMM and NCC display a selective BOLD activation pattern for the courtship compared to the non-courtship song suggests the involvement of these two regions in female preference for FD songs. One caveat with fMRI data, however, is that anesthesia is used during scanning, which could affect the gain and selectivity of auditory responses (e.g., [24, 25]). To provide additional verification of the effects seen with fMRI, we quantified the expression of the immediate early gene (IEG) EGR1 in the CMM and NCC after birds listened to FD or UD songs while awake as an alternative marker for neuronal activation.

In general, EGR1 expression in both the CMM and NCC mirrored the fMRI results (Figure 4). In the CMM, there was auditory-evoked EGR1 expression, with greater expression to song playback compared to silence (Figure 4A; Figure S2; $F_{(1,14.6)} = 33.3824$, $p < 0.0001$). In addition, EGR1 expression was significantly modulated by the stimulus ($F_{(1,9.1)} = 6.9585$; $p = 0.0267$) with significantly higher expression, bilaterally, in response to FD songs versus UD songs. As was the case for the BOLD fMRI response, in the NCC, there was no significant increase in EGR1 expression in response to song playback compared to silence ($F_{(1,10.2)} = 3.3582$, $p = 0.0962$). However, EGR1 expression was significantly influenced by the song stimulus ($F_{(1,10.7)} = 6.6228$, $p = 0.0264$), with higher expression in response to FD compared to UD song, which again parallels the fMRI results. Finally, in line with the results of the lateralization analysis of the fMRI data, EGR1 expression in the NCC was strongly lateralized, with significantly higher expression in the left compared to the right hemisphere ($F_{(1,4.6)} = 8.2804$, $p = 0.0379$).

The NCC Has Lower Tyrosine Hydroxylase$^+$-Fiber Density than the Neighboring Nidopallium

Through the fMRI and ICC data described above, we have uncovered a novel region within the caudocentral nidopallium that shows selective activation for preferred, socially modulated song. In a recently published songbird atlas, this region has been described as the caudolateral nidopallium (NCL), stemming from its location lateral to the secondary auditory region NCM [23]. In pigeons and crows, a portion of the NCL (which we will term the functional NCL) is significantly involved in executive functions, such as decision-making and higher-order multimodal processing, and is considered functionally analogous to the mammalian prefrontal cortex [26]. The NCL in pigeons was identified based on its connectivity, including a dense projection from midbrain tyrosine hydroxylase (TH^+) neurons [27]. In particular, compared to the surrounding nidopallium, the functional NCL contains more TH^+ fibers in general, as well as significantly more basket-like structures, visible as TH^+ fibers coiling up around large unstained perikarya (Figure 5C black arrows [28]). To investigate whether the FD-song-selective region that we identified using BOLD fMRI is comparable to the functional NCL in pigeons, we imaged the density of TH^+ fibers in the FD-song-selective region and surrounding nidopallium, including the NCM and dorsal and lateral caudal nidopallium (NC).

We observed clear variation in the density of TH^+ fibers and baskets throughout the NC at the rostro-caudal level of the ROI for our NCC fMRI signal (Figures 5A and 5B). The highest TH density, both in terms of fibers and baskets, was found in the most medial region, which corresponds to the most medial portions of the NCM (Figures 5B and 5C top) and stretches laterally to approximately 1 mm from the midline. In the central part of the NC directly lateral to the NCM (marked "NCL" in the Karten atlas [23]), we found two distinct areas based on their TH profile. A dorsal region, near the HVC, contained both TH baskets and TH^+-fiber innervation, although at lower levels than those observed in the NCM. Previous studies in zebra finches have referred to this region as dorsal NCL (dNCL) [29]. In contrast, a ventral region adjacent to the arcopallium, where our FD-song-selective region was located, was only sparsely innervated by TH^+ fibers and contained a low number of TH baskets (Figure 5C bottom). Based on this low level of TH^+ innervation and baskets, it appears that the FD-song-selective fMRI signal is not located in a functional NCL-like region [28]. We therefore identify this region as the NCC given its neuroanatomical location.

Neural Selectivity in the NCC Parallels Behavioral Responses to Modified FD Songs

Song-evoked activity, as measured by both fMRI and EGR1 expression, was modulated by the the stimulus in both the CMM and NCC. To gain further insight into how these two areas compare in function, we tested behavioral and neural responses to two novel stimuli that manipulated temporal and spectral song

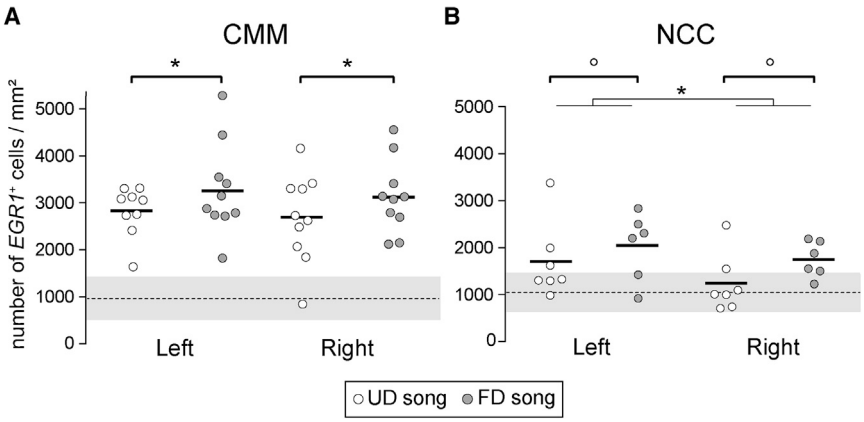

Figure 4. FD Song Elicits Greater EGR1 Expression than UD Song in Both the CMM and NCC

(A and B) The number of EGR1$^+$ neurons per square millimeter is significantly higher following FD song playback (green) than following UD song playback (blue) in the CMM (A) and the NCC (B). Points are individual females (see STAR Methods for more details on the sample sizes), dashed lines ± shaded areas represent the mean ± SD of the silence controls. Black horizontal bars represent the group mean.

Abbreviations: (FD) female directed; (UD) undirected; (CMM) caudomedial mesopallium; (NCC) caudocentral nidopallium. (*$p < 0.05$).

See also Figure S2.

features: mFD songs, which contained UD song syllables presented within the temporal structure of FD song; and mCTRL, which contained FD song syllables presented within the temporal structure of FD songs to control for the overall song manipulation and greater amplitude contrast of manipulated songs (Figure 6A).

We found striking differences in the BOLD fMRI responses between the CMM and NCC to the manipulated stimuli. In the right CMM, BOLD responses to FD and the manipulated stimuli were similar and significantly higher than responses to UD songs (FD > UD: $T_{max} = 3.0643$, $P_{FWE} = 0.0075$; mCTRL > UD: $T_{max} = 3.3138$, $P_{FWE}<0.0040$; mFD > UD: $T_{max} = 2.1620$, $P_{FWE} = 0.0538$; Figure 6B). In contrast, in the left NCC, we observed differential responses to the manipulated stimuli relative to the FD song. In particular, responses to FD were not only significantly higher than responses to UD songs, but were also significantly higher than either manipulated stimulus (FD > UD: $T_{max} = 3.2424$, $P_{FWE} = 0.0139$; FD > mCTRL: $T_{max} = 2.8184$, $P_{FWE} = 0.0367$; FD > mFD: $T_{max} = 2.8491$, $P_{FWE} = 0.0343$; Figure 6C). Thus, the CMM appears to respond to the manipulated stimuli as similar to FD song, while the NCC distinguishes FD songs from both the manipulated stimuli and UD songs.

To investigate whether CMM or NCC responses better correlate with behavioral perception of the manipulated stimuli, we tested females on FD, UD, and manipulated stimuli in a call-back assay. Behaviorally, females displayed dramatically different responses to the unmanipulated and manipulated stimuli, as indicated by the significant main effect of stimulus ($F_{(3,33)} = 3.0974$, $p = 0.0400$; Figure 6D). In particular, as has been seen in previous studies, females called significantly more to FD than UD songs ($p = 0.0287$ [13, 14];). In contrast, the preference for FD songs diminished with both types of song manipulation (manipulated songs versus UD songs: $p > 0.20$).

Not only were responses to the manipulated stimuli diminished relative to FD songs, they were also more variable. In particular, while females consistently increased calling to FD songs and decreased calling to UD songs, there was substantially more variation in the degree and direction of calling response to the manipulated stimuli. To further investigate this variation, we compared the rankings of responses to stimuli across females. For each female, we ranked the responses to each stimulus from most positive to most negative. As we had noted in the raw data, FD songs were more likely to receive the most positive response (FD songs were ranked "1" in 58% of the cases and were never ranked "4"; Figure S3). In contrast, the second, third, and fourth ranks were almost equally likely to be any of the other stimuli. Overall, we found that the pattern of rankings was significantly different for the FD song compared to the UD song (Cochran-Mantel-Haenszel $\chi^2 = 3.9302$, $p = 0.0474$) and the mCTRL stimulus (Cochran-Mantel-Haenszel $\chi^2 = 3.9302$, $p = 0.0474$), and there was a trend toward a difference for mFD stimuli (Cochran-Mantel-Haenszel $\chi^2 = 3.4571$, $p = 0.0630$; Figure S3). However, there were no significant differences between the rankings of UD songs and either manipulated stimulus ($p > 0.20$). The variation across birds in the responses to the manipulated stimuli indicates that females are sensitive to changes in auditory contrast or other subtle differences present in the manipulated stimuli, and furthermore, these data imply that females may not be categorizing the manipulated stimuli as FD songs.

DISCUSSION

In social species, communication signals convey substantial information about the identity, state, or quality of the signaler. During courtship, female receivers must accurately interpret male courtship signals to judge their relevance for mate choice and to compose the proper behavioral response. In zebra finches, females have been shown to be sensitive to subtle variation in male songs and to strongly prefer the longer, faster, and more stereotyped FD songs, performed by males in a courtship context, to UD songs, sung when males are alone [13, 14]. While the study of the songbird auditory system has identified regions that differentially respond to FD and UD songs in females [13, 14], the role of other forebrain regions in the discrimination and behavioral response to social-context-induced variation in the acoustic features of songs, as well as the link between auditory responses and behavioral preferences, remain poorly understood. Indeed, approaches used to study the neural basis of song discrimination and preference often require the *a priori* selection of regions of interest, an approach that is highly effective when used to study identified circuits, but not in uncovering novel regions of interest. Here, we employed BOLD fMRI, ICC of activity dependent proteins, and behavioral

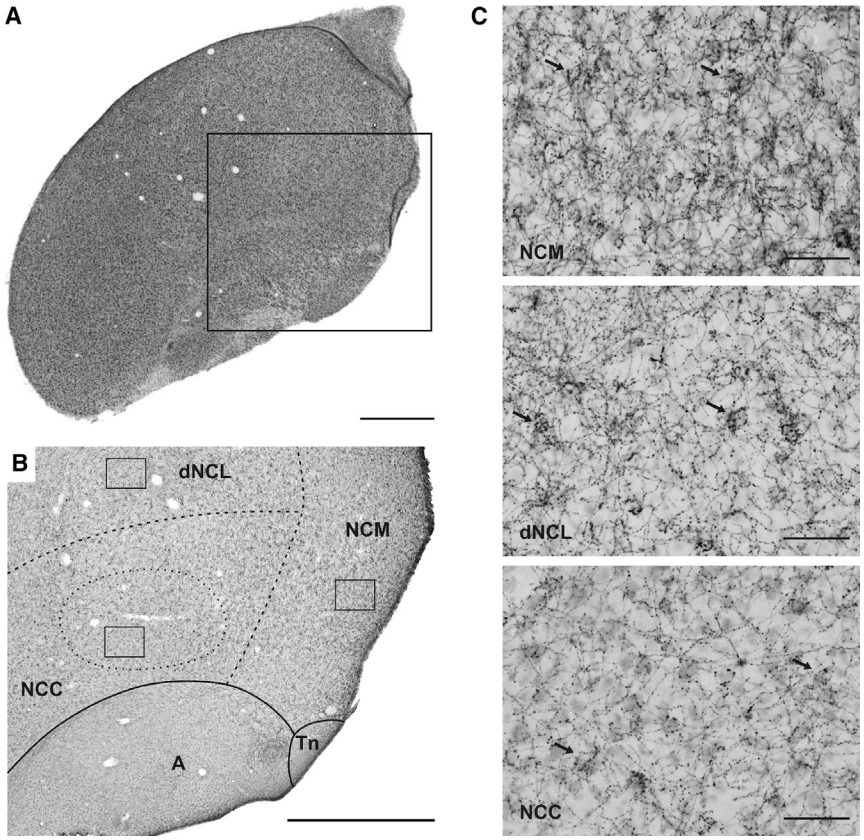

Figure 5. Differences in TH$^+$ Fiber and Basket Densities Indicate Subdivisions of the Caudal Nidopallium

TH density was measured within the NC at the level of the FD-selective NCC area.

(A) Nissl-stained overview image illustrating the coronal sections of interest (retrieved from the digital zebra finch brain atlas: http://zebrafinch.brainarchitecture.org [23]).

(B) Magnification (black square in [A]) of a representative TH stained section. Solid lines indicate known boundaries, dashed lines indicate putative region boundaries based on TH densities. Squares are the locations where TH$^+$ fiber density and number of baskets were quantified. The fMRI signal of the FD-song-selective region is indicated by the dashed circle located within the NCC.

(C) Differences in fiber density and morphology of baskets (black arrows) allow for an approximation of the borders of the NCM, NCL, and NCC (dashed lines in B). NCM can be characterized by dense innervation and a large number of highly innervated baskets (C, top) and extends approximately 1 mm from the midline. In contrast, dNCL shows fewer baskets and is moderately innervated by TH$^+$ fibers (middle). The NCC contains very few baskets and a low number of TH$^+$ fibers.

Abbreviations: (A) arcopallium; (NCM) caudomedial nidopallium; (NCC) caudocentral nidopallium; (dNCL) dorsal caudolateral nidopallium; (Tn) nucleus taeniae. Scale bar, 1000 μm in (A) and (B) and 50 μm in (C).

assays to uncover novel regions involved in song preference. Using fMRI, we identified two regions that differentially respond to FD and UD songs: the secondary auditory area CMM and a novel region in the caudal nidopallium, the NCC. In both regions, there was differential EGR1 expression in response to FD and UD songs, confirming the effects seen in the BOLD fMRI responses. Interestingly, we found that the two regions differed in their responses to manipulated stimuli. Relative to FD songs, the manipulated stimuli elicited diminished behavioral responses and BOLD fMRI signal in the NCC. These data hint that activity in the NCC may be more tightly coupled to the behavioral response and highlight the value of fMRI studies in songbirds for uncovering novel circuits important for perception and behavior.

We used acoustically manipulated stimuli, created by interchanging either FD or UD syllables into the temporal pattern of FD songs, to probe differences in the function of the CMM versus the NCC. The mFD stimuli thus contained UD spectral characteristics but FD temporal profiles, whereas the mCTRL stimuli contained both the spectral and temporal characteristics of FD songs. Through the manipulation process, we preserved the spectral characteristics of individual syllables, as well as the mean and variance of the durations of syllables and intersyllable intervals. However, both the mFD and mCTRL stimuli had greater amplitude contrast at syllable onsets and offsets than did the unmanipulated stimuli. Intriguingly, we observed that birds did not increase calling to either the mFD or the mCTRL stimulus indicating that the manipulation diminished behavioral preferences for FD song features. Moreover, whereas the FD songs received the most positive response from the majority of birds, the relative rankings of mFD, mCTRL, and UD songs were lower and more variable than the rankings of FD songs. Although, further song manipulations are clearly needed to tease apart the influences of spectrotemporal and amplitude features on song preference and perception, these data hint that the manipulated stimuli may be treated as categorically different from FD songs.

The behavioral responses are in striking contrast to the BOLD responses measured in the CMM, where both manipulated stimuli resulted in similar activation profiles as the unmanipulated FD stimuli. Previous studies comparing EGR1 expression in the CMM in response to salient or preferred songs, including FD songs in zebra finches, as well as in response to "sexy syllables" in canaries, have hypothesized that the CMM is significantly involved in discriminating song quality or salience [13, 30]. However, one challenge has been the difficulty in uncoupling differences in acoustic features from differences in preference. More recent work has demonstrated that EGR1 expression in the CMM does not directly correlate with behavioral responses [14, 31]. Such a lack of correlation between CMM response and behavior is similar to the effect that we report here, based on the responses to acoustically manipulated stimuli, where our data demonstrate that while neural responses in the CMM are indeed sensitive to differences between FD and UD songs in zebra finches, the neural modulation does not neatly parallel the behavioral relevance of changes in acoustic structure. In

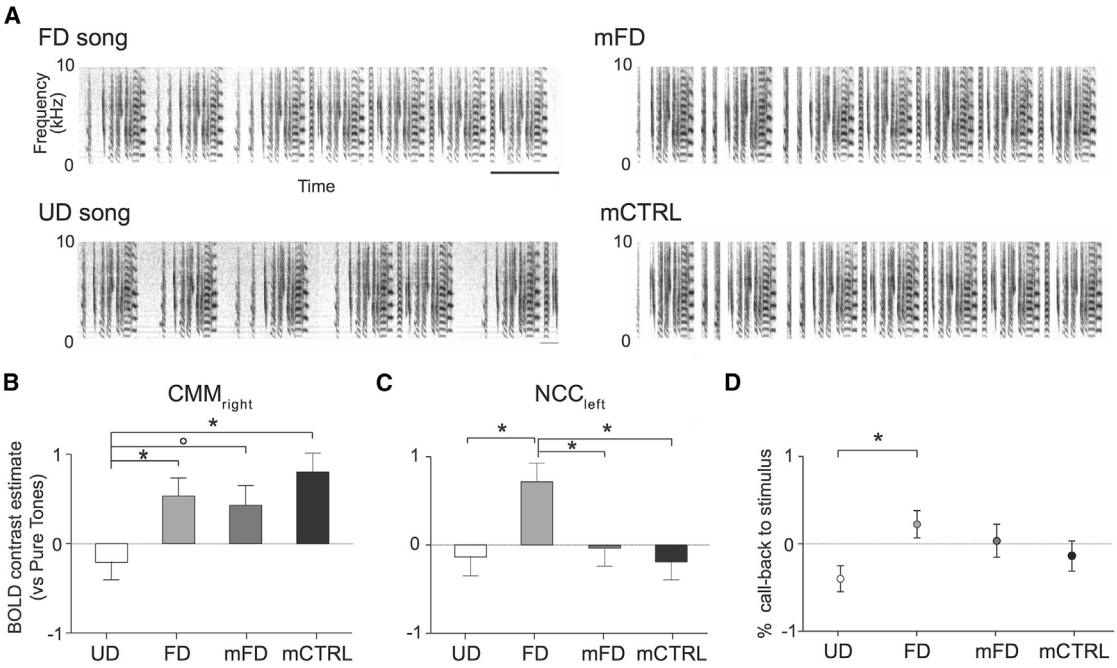

Figure 6. Responses to Acoustically Modified Versions of FD Songs Reveal Functional Differences between the CMM and the NCC

(A) Representative sound spectrograms for each stimulus type (excerpts from original 16 s long stimuli). Scale bar, 1 s.

(B and C) The average relative response amplitude (± SEM) of neural activations elicited by the different stimuli in the right CMM (B) and left NCC (C) (values from the voxel with the maximum t value for the main effect stimulus). The zero level corresponds to the estimated mean BOLD response relative to pure tones ($^{\circ}P_{FWE} < 0.1$; $^{*}P_{FWE} < 0.05$; n = 16).

(D) Percent change in calling (relative to the pre-stimulus period) in response to UD songs, FD songs, mFD songs, and mCTRL songs. Mean ± SEM ($^{*}p < 0.05$; n = 13).

Abbreviations: (FD) female directed song; (mFD) manipulated female directed song; (mCTRL) song stimulus controlling for manipulation; (UD) undirected song. See also Figure S3.

particular, we find that responses in the CMM are similar for FD songs, mFD songs that have the temporal aspects of FD songs but the spectral aspects of UD songs (mFD), and mCTRL songs, a control version of an FD song with greater amplitude contrast. As these three stimuli all share the same temporal features, we hypothesize that in the CMM, the temporal pattern of the song may be more important than spectral characteristics in driving the increased activation seen for FD versus UD songs. Note, however, that from the current results, it is unclear whether the greater activation in the CMM in response to FD songs is due to the increased tempo of FD relative to UD songs (e.g., shorter syllables) or due to greater song density (e.g., shorter inter-motif intervals). In either case, the hypothesis that temporal features are more important than spectral characteristics in driving CMM responses is supported by the earlier observation that EGR1 expression in the CMM is influenced by the temporal structure of song [32]. Moreover, temporal cues have been shown to be more important than spectral cues in the processing of auditory stimuli in the sensorimotor nucleus HVC (proper name [33]), which raises the possibility that auditory and sensorimotor forebrain circuits might be biased toward temporal features in this species in general [34].

Playback of FD songs also selectively increased BOLD responses in the NCC. To our knowledge, this is the first report of neural selectivity for socially modulated songs outside of the classical avian auditory pathway. Moreover, the pattern of activity in the NCC in response to the manipulated and unmanipulated stimuli was remarkably similar to the pattern of behavioral preferences. In particular, both calling behavior and the NCC BOLD responses were increased only in response to FD song playback. While it is difficult to determine precisely which acoustic features drive or suppress the response to FD songs, it is interesting to speculate that both FD selectivity in the NCC and behavioral preferences may require the preservation of intact songs with all spectral and temporal components in place and natural amplitude contrast at syllable on- and offsets. Additional studies that are more focused on elucidating the effect of spectral and temporal variability on neural selectivity, and on how this correlates with behavioral preference, will be key in understanding how females weigh specific acoustic features when determining song quality and what role the NCC in particular plays in this process. Moreover, one significant caveat in the comparison of the fMRI and behavioral data is the difference in behavioral state: fMRI is performed on anesthetized birds, while birds are awake for behavioral tests. Such changes in state may significantly affect the gain, latency, and tuning of neural responses [24, 25, 35–37]. That said, the observed parallels between responses in the NCC and behavioral preferences in this study raise the intriguing possibility that the NCC may be significant in driving behavioral responses to songs.

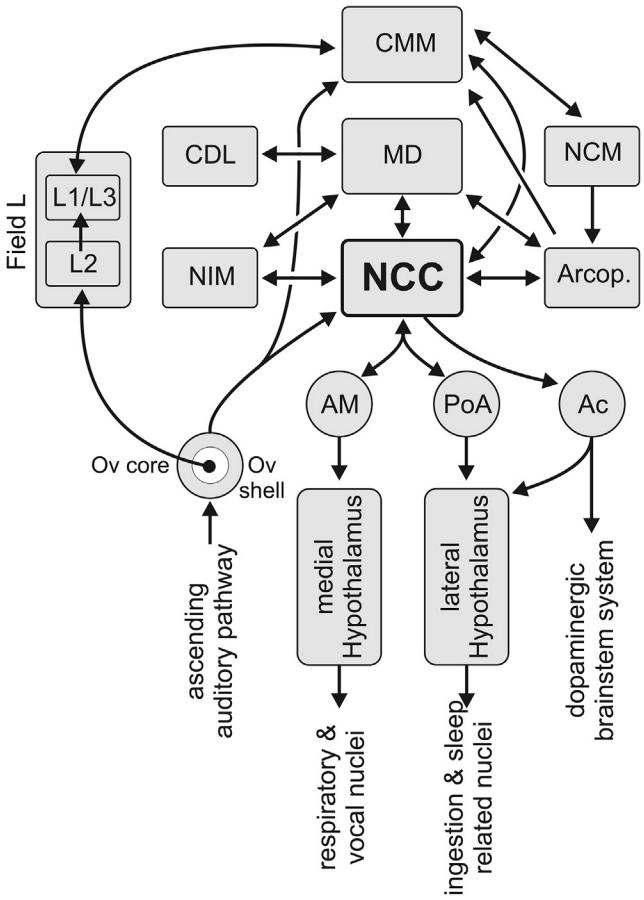

Figure 7. Suggested Overview of NCC Connectivity Related to FD Song Processing and Courtship Behavior

The caudocentral nidopallium (NCC) receives direct auditory input from the shell of the nucleus ovoidalis (Ov shell) and indirect input from the caudomedial mesopallium (CMM) and caudomedial nidopallium (NCM) via the multimodal arcopallium [38–40]. It also has reciprocal connections with the intermediate medial nidopallium (NIM), a part of a frontal medial region for filial imprinting based on visual and auditory stimuli [41, 42]. In addition, the NCC has reciprocal connections with the limbic dorsomedial mesopallium (MD) that integrates various sensory streams and communicates via the dorsolateral corticoid area (CDL) with the hippocampus [38]. The NCC has three important descending projections: through the nucleus accumbens (Ac) to putatively dopaminergic midbrain cell groups, through the posterior nucleus of the pallial amygdala (PoA) and Ac to the lateral hypothalamus, and through the medial arcopallium (AM) to the medial hypothalamus [38, 43]. Through these connections, the NCC gains access to reward circuitry (via the Ac and dopaminergic midbrain nuclei), ingestion- and sleep-related nuclei (via PoA and Ac connections to the lateral hypothalamus), and respiratory and vocal nuclei (via AM to medial hypothalamus) [38, 43–45].

Abbreviations: (Ac) nucleus accumbens; (AM) medial arcopallium; (Acrop.) arcopallium; (CDL) dorsolateral corticoid area; (CMM) caudomedial mesopallium; (DM) dorsomedial nucleus of the midbrain; (MD) dorsal mesopallium; (NCC) caudocentral nidopallium; (NCM) caudomedial nidopallium; (NIM) intermediate medial nidopallium; (Ov shell) shell of the nucleus ovoidalis; (PoA) posterior nucleus of the pallial amygdala.

The region we identify as the NCC in our fMRI images is located centrally in the caudal nidopallium and exhibits lower levels of TH innervation than the surrounding nidopallium, including the NCM and the dNCL. To our knowledge, there are no specific reports describing the function or connectivity of this region either in zebra finches or in any other songbird species. However, both the neuroanatomical position and TH innervation profile of the identified FD-song-selective region are similar to the NCC, a higher-order limbic forebrain area that has been described in a non-songbird avian species, the pigeon [38]. In particular, the connectivity of this region has been well-characterized in pigeons (Figure 7) and indicates that the NCC may be involved in multiple facets of courtship behavior, including coordinating auditory inputs, memory from sexual imprinting structures, and vocal and behavioral responses to courtship signals [38–45]. The NCC receives auditory input from both the shell of the auditory thalamic nucleus ovoidalis (Ov shell) and the secondary cortical region NCM (via the multimodal arcopallium), which is highly interconnected with the CMM and the primary auditory forebrain [39]. In addition, the NCC is reciprocally connected to regions that are implicated in learning and memory associated with sexual imprinting, such as the intermediate medial nidopallium (NIM) and the limbic dorsal mesopallium (MD) [41, 42]. Together, the connections to auditory and imprinting structures raise the possibility that the NCC is a hub for the memorization and integration of auditory and other sensory input which can influence mate choice in adult zebra finches [41, 42]. Finally, the NCC also connects to parts of the arcopallium with descending projections to motor output regions, which may enable the NCC to modify behavioral responses [44]. In particular, with regard to our behavioral assay, the NCC projects to the medial arcopallium (AM), which connects to the dorsomedial nucleus (DM) of the midbrain via the posterior medial hypothalamus [44]. The DM can control brainstem respiratory and vocal nuclei, and parts of DM have been shown to be involved in the control of female reproductive behavior, including copulation solicitation displays [39, 45, 46]. Consequently, DM is a key structure that could drive callback responses, as well as increase copulation solicitation displays to preferred songs. Thus, the connectivity of the NCC positions it as an integrative hub, potentially important for evaluating courtship signals and coordinating a multi-faceted behavioral response. Our fMRI results, documenting a correlation between neuronal responses in the NCC and behavioral callback responses to acoustic stimuli, provide, to our knowledge, the first functional support of such a role for the NCC in the evaluation of courtship signals and in coordinating resulting behavioral responses in female zebra finches.

The two independent techniques we used to infer neural activity each provide discrete, indirect measures of changes in neuronal firing. Moreover, although fMRI and EGR1 expression methods differ substantially in the physiological events they measure, the time course for activation to be detected, and the wakefulness of the animals during auditory stimulation, both methods indicated that activity in the CMM and NCC is modulated by social-context-induced song variation. Thus, despite these methodological differences and in line with previous observations [20], the selectivity of the regions localized using *in vivo* fMRI could be validated using the *ex vivo* technique. One substantial difference, however, is that significant lateralization of FD song selectivity was apparent only in the results of the fMRI experiment. For the NCC, FD-selective BOLD responses

were only detected in the left hemisphere. However, overall, responses to both stimuli were higher in the left than the right hemisphere. Thus, it is also possible that the lack of a difference in responses to FD and UD songs in the right hemisphere arises not because of functional lateralization but due to an overall lower level of activation. Lateralized manipulations of activity in the NCC will prove interesting to understanding the degree of lateralization of this region. In contrast, the overall level of activation was similar in the two hemispheres in the CMM for both techniques. Consequently, the lack of selective BOLD responses in the left CMM is likely not due to lower sensitivity but rather is indicative of functional lateralization. More research on the nature of lateralized responses to songs in the auditory forebrain and the effect of anesthesia are necessary to fully understand the discrepancies in responses between the two techniques.

In humans, there is well-established lateralization of language to the left hemisphere. However, additionally, there is substantial variation in the degree and direction of lateralization for perception of characteristics of speech—for example, vocal prosodic features, including spectral and temporal characteristics that vary with emotional content [47–49]. In particular, it is hypothesized that the right hemisphere may be more significant in lower-order processing of complex auditory stimuli, while the left hemisphere is significant for the higher-order processing of internal representations [49]. These data provide an interesting parallel to the differences we describe here in hemispheric dominance between the CMM (right dominant) and NCC (left dominant) in songbirds, especially given potential similarities in the function and types of variation in acoustic features between FD and UD songs and prosodic changes in speech. Moreover, there is considerable debate as to whether hemispheric differences arise from higher-order areas feeding back into auditory cortical regions (top-down influences) or whether they arise from inherent, hemispheric differences in the spectrotemporal resolution in the auditory cortex (bottom-up [48]). In songbirds, a number of the inputs to the CMM and NCC show hemispheric dominance, including the NCM and the MD. In the NCM, which provides input to both the CMM and NCC, the dominant hemisphere appears to vary depending on the nature of the stimulus and the auditory experience of the bird [50–52]. Circuit-breaking experiments in songbirds may help to provide better insight into the types of circuit-level interactions that contribute to hemispheric differences in the processing of complex, behaviorally relevant, auditory stimuli.

To date, little is known about the function of regions in the caudocentral nidopallium, including the NCC, beyond what has been postulated based on connectivity. However, one of the few functional studies has implicated a region posterior to the NCC in male courtship behavior [53–55]. In particular, a region within the central part of the caudal nidopallium (referred to as the caudal arcopallium/nidopallium, "ANC") that lies just caudal to the NCC exhibits increased 2-deoxyglucose expression following courtship behavior in male zebra finches [55]. Meanwhile, our data reveal that responses in the NCC are directly correlated to behavioral call-back responses in female zebra finches. Further study is necessary to elucidate whether the NCC and ANC represent sex-specific specializations of the caudocentral nidopallium, differentially important for courtship behavior and sexual decision making in males and females. However, our data suggest that the NCC in female finches is important for evaluating and coordinating responses to socially modulated acoustic signals and raises the possibility that the NCC serves as an integrative hub for sensory and motor connections important in vocal communication and mate choice.

STAR★METHODS

Detailed methods are provided in the online version of this paper and include the following:

- KEY RESOURCES TABLE
- CONTACT FOR REAGENT AND RESOURCE SHARING
- EXPERIMENTAL MODEL AND SUBJECT DETAILS
- METHOD DETAILS
  - Auditory Stimuli
  - Functional MRI
  - EGR1 expression
  - TH expression
  - Call-back behavior
- QUANTIFICATION AND STATISTICAL ANALYSIS
  - fMRI group analysis
  - EGR1 expression analysis
  - Call-back analysis
- DATA AND SOFTWARE AVAILABILITY

SUPPLEMENTAL INFORMATION

Supplemental Information includes three figures and one table and can be found with this article online at https://doi.org/10.1016/j.cub.2018.01.048.

ACKNOWLEDGMENTS

We thank Vivian Ng and Michele Kim for their help in collecting the behavioural data and Gaurav Majumdar and Garima Yadav for their assistance in sample preparation for the TH IC. This research was supported by grants from the Research Foundation – Flanders (FWO, Project No. G030213N and G044311N), the Hercules Foundation (Grant No. AUHA0012), and Interuniversity Attraction Poles (IAP) ('PLASTOsCINE': P7/17) to A.V.d.L., grants from the German Research Foundation (DGN, Project No. SFB 874 and Gu227/16-1) to O.G., and grants from the National Sciences and Engineering Research Council (Project No. RGPIN402186 and RGPIN402417 [main grant holder: Jon Sakata]) to S.C.W. L.V.R. and J.H. are PhD fellows supported by the FWO and the University of Antwerp, respectively.

AUTHOR CONTRIBUTIONS

Conceived and designed the experiments: L.V.R., S.C.W., and A.V.d.L.; Performed the fMRI experiments: L.V.R.; performed the behavioral and EGR1 ICC experiments: Y.C. and S.C.W.; performed the TH immunostaining: K.v.E. and O.G.; Performed final data analysis: L.V.R.; Advised on and contributed to data analysis: J.H., G.D.G, M.V., Y.C., and S.C.W.; Contributed reagents, materials and/or analysis tools: O.G., S.C.W., and A.V.d.L.; Contributed to data interpretation: L.V.R., O.G., S.C.W., and A.V.d.L.; Wrote the paper: L.V.R., O.G., S.C.W., and A.V.d.L. All authors critically reviewed the manuscript; S.C.W. and A.V.d.L. approved the final version of the manuscript.

DECLARATION OF INTEREST

The authors declare no competing interests.

Received: August 15, 2017
Revised: December 5, 2017
Accepted: January 17, 2018
Published: February 22, 2018

REFERENCES

1. Andersson, M. (1994). Sexual Selection (Princeton, New Jersey: Princeton University Press).
2. Bradbury, J., and Vehrencamp, S. (1998). Principles of animal communication (Sunderland: Sinauer Associates).
3. Rosenthal, G.G. (2017). Mate Choice: The Evolution of Sexual Decision Making from Microbes to Humans (Princeton University Press).
4. Ryan, M. (1985). The tungara frog: a study in sexual selection and communication (Chicago: Univ. Chicago Press).
5. Akre, K.L., Farris, H.E., Lea, A.M., Page, R.A., and Ryan, M.J. (2011). Signal perception in frogs and bats and the evolution of mating signals. Science *333*, 751–752.
6. West, M.J., and King, A.P. (1988). Female visual displays affect the development of male song in the cowbird. Nature *334*, 244–246.
7. Zann, R.A. (1996). The zebra finch: A synthesis of field and laboratory studies (Oxford: Oxford University Press).
8. Brainard, M.S., and Doupe, A.J. (2002). What songbirds teach us about learning. Nature *417*, 351–358.
9. Mooney, R. (2009). Neurobiology of song learning. Curr. Opin. Neurobiol. *19*, 654–660.
10. Riebel, K. (2009). Song and Female Mate Choice in Zebra Finches: A Review. In Advances in the Study of Behavior, *Volume 40* (Academic Press), pp. 197–238.
11. Clayton, N.S. (1988). Song discrimination learning in zebra finches. Anim. Behav. *36*, 1016–1024.
12. Miller, D.B. (1979). The acoustic basis of mate recognition by female Zebra finches (*Taeniopygia guttata*). Anim. Behav. *27*, 376–380.
13. Woolley, S.C., and Doupe, A.J. (2008). Social context-induced song variation affects female behavior and gene expression. PLoS Biol. *6*, e62.
14. Chen, Y., Clark, O., and Woolley, S.C. (2017). Courtship song preferences in female zebra finches are shaped by developmental auditory experience. Proc. Biol. Sci. *284*.
15. Van Ruijssevelt, L., Van der Kant, A., De Groof, G., and Van der Linden, A. (2013). Current state-of-the-art of auditory functional MRI (fMRI) on zebra finches: technique and scientific achievements. J. Physiol. Paris *107*, 156–169.
16. Van Ruijssevelt, L., De Groof, G., Van der Kant, A., Poirier, C., Van Audekerke, J., Verhoye, M., and Van der Linden, A. (2013). Functional magnetic resonance imaging (FMRI) with auditory stimulation in songbirds. J. Vis. Exp. *3*.
17. Voss, H.U., Tabelow, K., Polzehl, J., Tchernichovski, O., Maul, K.K., Salgado-Commissariat, D., Ballon, D., and Helekar, S.A. (2007). Functional MRI of the zebra finch brain during song stimulation suggests a lateralized response topography. Proc. Natl. Acad. Sci. USA *104*, 10667–10672.
18. Van Meir, V., Boumans, T., De Groof, G., Van Audekerke, J., Smolders, A., Scheunders, P., Sijbers, J., Verhoye, M., Balthazart, J., and Van der Linden, A. (2005). Spatiotemporal properties of the BOLD response in the songbirds' auditory circuit during a variety of listening tasks. Neuroimage *25*, 1242–1255.
19. Boumans, T., Theunissen, F.E., Poirier, C., and Van Der Linden, A. (2007). Neural representation of spectral and temporal features of song in the auditory forebrain of zebra finches as revealed by functional MRI. Eur. J. Neurosci. *26*, 2613–2626.
20. Boumans, T., Vignal, C., Smolders, A., Sijbers, J., Verhoye, M., Van Audekerke, J., Mathevon, N., and Van der Linden, A. (2008). Functional magnetic resonance imaging in zebra finch discerns the neural substrate involved in segregation of conspecific song from background noise. J. Neurophysiol. *99*, 931–938.
21. Poirier, C., Verhoye, M., Boumans, T., and Van der Linden, A. (2010). Implementation of spin-echo blood oxygen level-dependent (BOLD) functional MRI in birds. NMR Biomed. *23*, 1027–1032.
22. Poirier, C., Vellema, M., Verhoye, M., Van Meir, V., Wild, J.M., Balthazart, J., and Van Der Linden, A. (2008). A three-dimensional MRI atlas of the zebra finch brain in stereotaxic coordinates. Neuroimage *41*, 1–6.
23. Karten, H.J., Brzozowska-Prechtl, A., Lovell, P.V., Tang, D.D., Mello, C.V., Wang, H., and Mitra, P.P. (2013). Digital atlas of the zebra finch (Taeniopygia guttata) brain: a high-resolution photo atlas. J. Comp. Neurol. *521*, 3702–3715.
24. Karino, G., George, I., Loison, L., Heyraud, C., De Groof, G., Hausberger, M., and Cousillas, H. (2016). Anesthesia and brain sensory processing: impact on neuronal responses in a female songbird. Sci. Rep. *6*, 39143.
25. Gaese, B.H., and Ostwald, J. (2001). Anesthesia changes frequency tuning of neurons in the rat primary auditory cortex. J. Neurophysiol. *86*, 1062–1066.
26. Güntürkün, O. (2005). The avian 'prefrontal cortex' and cognition. Curr. Opin. Neurobiol. *15*, 686–693.
27. Waldmann, C., and Güntürkün, O. (1993). The dopaminergic innervation of the pigeon caudolateral forebrain: immunocytochemical evidence for a 'prefrontal cortex' in birds? Brain Res. *600*, 225–234.
28. Wynne, B., and Güntürkün, O. (1995). Dopaminergic innervation of the telencephalon of the pigeon (Columba livia): a study with antibodies against tyrosine hydroxylase and dopamine. J. Comp. Neurol. *357*, 446–464.
29. Bottjer, S.W., Brady, J.D., and Cribbs, B. (2000). Connections of a motor cortical region in zebra finches: relation to pathways for vocal learning. J. Comp. Neurol. *420*, 244–260.
30. Leitner, S., Voigt, C., Metzdorf, R., and Catchpole, C.K. (2005). Immediate early gene (ZENK, Arc) expression in the auditory forebrain of female canaries varies in response to male song quality. J. Neurobiol. *64*, 275–284.
31. Gobes, S.M., Ter Haar, S.M., Vignal, C., Vergne, A.L., Mathevon, N., and Bolhuis, J.J. (2009). Differential responsiveness in brain and behavior to sexually dimorphic long calls in male and female zebra finches. J. Comp. Neurol. *516*, 312–320.
32. Lampen, J., Jones, K., McAuley, J.D., Chang, S.E., and Wade, J. (2014). Arrhythmic song exposure increases ZENK expression in auditory cortical areas and nucleus taeniae of the adult zebra Finch. PLoS ONE *9*, e108841.
33. Theunissen, F.E., and Doupe, A.J. (1998). Temporal and spectral sensitivity of complex auditory neurons in the nucleus HVc of male zebra finches. J. Neurosci. *18*, 3786–3802.
34. Woolley, S.M., Fremouw, T.E., Hsu, A., and Theunissen, F.E. (2005). Tuning for spectro-temporal modulations as a mechanism for auditory discrimination of natural sounds. Nat. Neurosci. *8*, 1371–1379.
35. Cardin, J.A., and Schmidt, M.F. (2003). Song system auditory responses are stable and highly tuned during sedation, rapidly modulated and unselective during wakefulness, and suppressed by arousal. J. Neurophysiol. *90*, 2884–2899.
36. Schumacher, J.W., Schneider, D.M., and Woolley, S.M.N. (2011). Anesthetic state modulates excitability but not spectral tuning or neural discrimination in single auditory midbrain neurons. J. Neurophysiol. *106*, 500–514.
37. Narayan, R., Graña, G., and Sen, K. (2006). Distinct time scales in cortical discrimination of natural sounds in songbirds. J. Neurophysiol. *96*, 252–258.
38. Atoji, Y., and Wild, J.M. (2009). Afferent and efferent projections of the central caudal nidopallium in the pigeon (Columba livia). J. Comp. Neurol. *517*, 350–370.
39. Wild, J.M., Karten, H.J., and Frost, B.J. (1993). Connections of the auditory forebrain in the pigeon (Columba livia). J. Comp. Neurol. *337*, 32–62.
40. Wild, J.M. (1993). The avian nucleus retroambigualis: a nucleus for breathing, singing and calling. Brain Res. *606*, 319–324.

41. Horn, G. (2004). Pathways of the past: the imprint of memory. Nat. Rev. Neurosci. *5*, 108–120.
42. Thode, C., Bock, J., Braun, K., and Darlison, M.G. (2005). The chicken immediate-early gene ZENK is expressed in the medio-rostral neostriatum/hyperstriatum ventrale, a brain region involved in acoustic imprinting, and is up-regulated after exposure to an auditory stimulus. Neuroscience *130*, 611–617.
43. Husband, S.A., and Shimizu, T. (2011). Calcium-binding protein distributions and fiber connections of the nucleus accumbens in the pigeon (Columba livia). J. Comp. Neurol. *519*, 1371–1394.
44. Zeier, H., and Karten, H.J. (1971). The archistriatum of the pigeon: organization of afferent and efferent connections. Brain Res. *31*, 313–326.
45. Wild, J.M., Li, D., and Eagleton, C. (1997). Projections of the dorsomedial nucleus of the intercollicular complex (DM) in relation to respiratory-vocal nuclei in the brainstem of pigeon (Columba livia) and zebra finch (Taeniopygia guttata). J. Comp. Neurol. *377*, 392–413.
46. Wild, J.M., and Botelho, J.F. (2015). Involvement of the avian song system in reproductive behaviour. Biol. Lett. *11*, 20150773.
47. Kotz, S.A., Meyer, M., and Paulmann, S. (2006). Lateralization of emotional prosody in the brain: an overview and synopsis on the impact of study design. Prog. Brain Res. *156*, 285–294.
48. Liebenthal, E., Silbersweig, D.A., and Stern, E. (2016). The Language, Tone and Prosody of Emotions: Neural Substrates and Dynamics of Spoken-Word Emotion Perception. Front. Neurosci. *10*, 506.
49. Gandour, J., Tong, Y., Wong, D., Talavage, T., Dzemidzic, M., Xu, Y., Li, X., and Lowe, M. (2004). Hemispheric roles in the perception of speech prosody. Neuroimage *23*, 344–357.
50. Bell, B.A., Phan, M.L., and Vicario, D.S. (2015). Neural responses in songbird forebrain reflect learning rates, acquired salience, and stimulus novelty after auditory discrimination training. J. Neurophysiol. *113*, 1480–1492.
51. Moorman, S., Gobes, S.M., Kuijpers, M., Kerkhofs, A., Zandbergen, M.A., and Bolhuis, J.J. (2012). Human-like brain hemispheric dominance in birdsong learning. Proc. Natl. Acad. Sci. USA *109*, 12782–12787.
52. Phan, M.L., and Vicario, D.S. (2010). Hemispheric differences in processing of vocalizations depend on early experience. Proc. Natl. Acad. Sci. USA *107*, 2301–2306.
53. Sadananda, M., and Bischof, H.J. (2002). Enhanced fos expression in the zebra finch (Taeniopygia guttata) brain following first courtship. J. Comp. Neurol. *448*, 150–164.
54. Sadananda, M., Korte, S., and Bischof, H.J. (2007). Afferentation of a caudal forebrain area activated during courtship behavior: a tracing study in the zebra finch (Taeniopygia guttata). Brain Res. *1184*, 108–120.
55. Bischof, H.J., and Herrmann, K. (1986). Arousal enhances [14C]2-deoxyglucose uptake in four forebrain areas of the zebra finch. Behav. Brain Res. *21*, 215–221.
56. Schubloom, H.E., and Woolley, S.C. (2016). Variation in social relationships relates to song preferences and EGR1 expression in a female songbird. Dev. Neurobiol. *76*, 1029–1040.
57. Tchernichovski, O. (1991). Sound Analysis Pro. Version 2, June 1991 Edition (Boston, MA: Free Software Foundation, Inc.).
58. Tchernichovski, O., Nottebohm, F., Ho, C.E., Pesaran, B., and Mitra, P.P. (2000). A procedure for an automated measurement of song similarity. Anim. Behav. *59*, 1167–1176.
59. Jarvis, E.D., Scharff, C., Grossman, M.R., Ramos, J.A., and Nottebohm, F. (1998). For whom the bird sings: context-dependent gene expression. Neuron *21*, 775–788.
60. Kao, M.H., and Brainard, M.S. (2006). Lesions of an avian basal ganglia circuit prevent context-dependent changes to song variability. J. Neurophysiol. *96*, 1441–1455.
61. Poirier, C., Boumans, T., Vellema, M., De Groof, G., Charlier, T.D., Verhoye, M., Van der Linden, A., and Balthazart, J. (2011). Own song selectivity in the songbird auditory pathway: suppression by norepinephrine. PLoS ONE *6*, e20131.
62. Poirier, C., Boumans, T., Verhoye, M., Balthazart, J., and Van der Linden, A. (2009). Own-song recognition in the songbird auditory pathway: selectivity and lateralization. J. Neurosci. *29*, 2252–2258.
63. van der Kant, A., Derégnaucourt, S., Gahr, M., Van der Linden, A., and Poirier, C. (2013). Representation of Early Sensory Experience in the Adult Auditory Midbrain: Implications for Vocal Learning. PLoS One *8*, e61764.82.-59.
64. Mello, C.V., and Ribeiro, S. (1998). ZENK protein regulation by song in the brain of songbirds. J. Comp. Neurol. *393*, 426–438.
65. Matheson, L.E., and Sakata, J.T. (2015). Catecholaminergic contributions to vocal communication signals. Eur. J. Neurosci. *41*, 1180–1194.
66. Matheson, L.E., Sun, H., and Sakata, J.T. (2016). Forebrain circuits underlying the social modulation of vocal communication signals. Dev. Neurobiol. *76*, 47–63.
67. Bharati, I.S., and Goodson, J.L. (2006). Fos responses of dopamine neurons to sociosexual stimuli in male zebra finches. Neuroscience *143*, 661–670.
68. Stacho, M., Letzner, S., Theiss, C., Manns, M., and Güntürkün, O. (2016). A GABAergic tecto-tegmento-tectal pathway in pigeons. J. Comp. Neurol. *524*, 2886–2913.
69. Shu, S.Y., Ju, G., and Fan, L.Z. (1988). The glucose oxidase-DAB-nickel method in peroxidase histochemistry of the nervous system. Neurosci. Lett. *85*, 169–171.
70. Jiao, Y., Sun, Z., Lee, T., Fusco, F.R., Kimble, T.D., Meade, C.A., Cuthbertson, S., and Reiner, A. (1999). A simple and sensitive antigen retrieval method for free-floating and slide-mounted tissue sections. J. Neurosci. Methods *93*, 149–162.
71. Bottjer, S.W. (1993). The distribution of tyrosine hydroxylase immunoreactivity in the brains of male and female zebra finches. J. Neurobiol. *24*, 51–69.
72. Sathyanesan, A., Ogura, T., and Lin, W. (2012). Automated measurement of nerve fiber density using line intensity scan analysis. J. Neurosci. Methods *206*, 165–175.
73. Rutstein, A.N., Brazill-Boast, J., and Griffith, S.C. (2007). Evaluating mate choice in the zebra finch. Anim. Behav. *74*, 1277–1284.
74. Dunning, J.L., Pant, S., Bass, A., Coburn, Z., and Prather, J.F. (2014). Mate choice in adult female Bengalese finches: females express consistent preferences for individual males and prefer female-directed song performances. PLoS ONE *9*, e89438.

STAR★METHODS

KEY RESOURCES TABLE

REAGENT or RESOURCE	SOURCE	IDENTIFIER
Antibodies		
Rabbit anti-EGR1	Santa Cruz Biotechnology	Cat# SC-189; RRID: AB_2231020
Sheep anti-tyrosine hydroxylase	Novus Biologicals, Littleton, CO, USA	Cat# NB300-110; RRID: AB_10002491
Mouse anti-NeuN	EMD Millipore, Billerica, MA, USA	Cat# MAB377; RRID: AB_2298772
Mouse anti-Tyrosine Hydroxylase Antibody (clone 2/40/15)	Merck-Millipore	Cat # MAB5280, Lot#2807054; RRID: AB_2201526
Biological Samples		
Female zebra finch brains	Woolley Laboratory, McGill University	N/A
Critical Commercial Assays		
Vectastain Elite ABC-HRP Kit (Peroxidase, Mouse IgG)	Vector Laboratories	Cat # PK-6102; RRID: AB_2336821
Experimental Models: Organisms/Strains		
Zebra finch *Taeniopygia guttata*	local registered breeder	Not applicable
Software and Algorithms		
Statistical parametric mapping	Wellcome Trust Centre for NeuroImaging	http://www.fil.ion.ucl.ac.uk/spm/
SPSS Statistics for Windows (Version 22.0. Armonk, NY: IBM)	IBM	https://www.ibm.com/products/spss-statistics
JMP 11.2.0	SAS Institute, Cary, NC	N/A
MATLAB	Mathworks, Natick MA	N/A
Fiji	NIH [1];	https://fiji.sc/
FeatureJ hessian-based filter	Meijering, E. (2003). FeatureJ: A Java package for image feature extraction	https://imagescience.org/meijering/software/featurej/

CONTACT FOR REAGENT AND RESOURCE SHARING

Further information and requests for resources and reagents should be directed to and will be fulfilled by the Lead Contact, Annemie Van der Linden (Annemie.vanderlinden@uantwerp.be).

EXPERIMENTAL MODEL AND SUBJECT DETAILS

We used adult zebra finches (*Taeniopygia Guttata*, > 90 days old) which were either purchased from registered breeders (Exotic Wings and Pet Things, St. Clements, Ontario, Canada) or bred at the local animal facility (McGill University, Montreal, QC, Canada; Bio-Imaging lab, University of Antwerp, Antwerp, Belgium; See Table S1 for an overview of the sample sizes per experiment). The fMRI experiments were performed at the Bio-Imaging lab, University of Antwerp (Belgium) where the birds were housed in large aviaries under a 12 hr light/dark cycle with access to food and water *ad libitum*. The birds for the TH immunostaining were also raised in these conditions before sacrifice. The behavioral experiments and the ICC analysis of EGR1 expression were performed at the Department of Biology, McGill University (Canada) on a separate group of birds which were housed in single-sex group cages (43 × 43 × 43 cm; < 10 birds/cage) prior to testing. Birds were maintained on a 14 hr light/10 hr dark photoperiod and provided with food and water *ad libitum* throughout the experiments. All procedures were approved by either the University of Antwerp ethical committee (License number: 2012-43) in agreement with the Belgian laws on the protection and welfare of animals (fMRI and TH ICC experiments) or the McGill University Animal Care and Use Committee and in accordance with the guidelines of the Canadian Council on Animal Care (behavior and EGR1 ICC).

METHOD DETAILS

Auditory Stimuli

Song recordings

Stimuli were FD and UD song from five different males ('stimulus males') that were unfamiliar and unrelated to the experimental females. Songs were recorded as previously described [13, 56]. Briefly, males were housed individually in a cage inside a

sound-attenuating chamber ('soundbox'; TRA Acoustics, Cornwall, Ontario) containing a microphone (Countryman Associates, California) and a video camera (PalmVid, Colorado). Vocalizations were recorded using a custom written sound-activated recording system (44.1 kHz) or Sound Analysis Pro (SAP [57, 58];) To collect FD song, we placed a cage containing a muted female next to the male's cage in the soundbox and monitored the male's behavior on a video monitor. During courtship song performance, males orient toward the female, fluff the body feathers while flattening feathers on top of the head, hop, dance, and beak wipe [7, 13, 59, 60].). Only songs where males performed at least two of the above courtship components were considered to be FD songs. Males performed one to two bouts of song for each female presentation. After removing the female, we waited up to 10 min before reintroducing the female in order to collect interleaved bouts of UD song. We also recorded an additional one hr of UD song before the first and after the last female presentation on each recording day. Males were recorded in the morning and were recorded over multiple days in order to ensure a sufficient number of FD song bouts to use for stimuli.

Muting was performed by placing a small piece of plastic tubing inside the bronchii as described in [13]. Briefly, following anesthesia (Equithesin 3.0-4.0 μg/g) we made small incisions in the skin and air sac to expose the syrinx. We then made an incision along the midline of the syrinx and placed a small piece of plastic tubing into each bronchia. The incision in the syrinx was closed using Nexaband (Abbott Animal Health) and the skin incision was closed with suture. The females that were used to elicit FD song for the recordings were not included in the remaining experiments.

Stimulus design

For the ICC experiments, we created FD and UD stimulus sets from the song recordings of each of five different males based on approaches previously used in our lab (e.g., [13, 14]). Zebra finch song is composed of individual acoustic elements or ''syllables,'' separated by at least 5 ms of silence, which are performed in a stereotyped sequence ('motif'). Males typically perform bouts of song, which are strings of motifs, preceded by short, simple syllables known as introductory notes. We used song bouts as stimuli, and defined each bout as an epoch of continuous sound that contained periods of silence shorter than 800 ms. Thus, each song bout contained multiple 'motifs' as well as introductory syllables. To select song bouts for use as stimuli, we used an automated amplitude-based segmentation algorithm custom-written in MATLAB (Mathworks, Natick, MA) to determine syllable boundaries for all syllables in all of our song recordings for each male. Every syllable was given an identifying label that we then used to determine the syllable sequence within a motif as well as the number of introductory notes, call notes, complete motifs, and incomplete motifs in all of the recorded song bouts. Based on these measures, we selected five to seven examples each of FD and UD song bouts from each male's repertoire to be used as stimuli. We used multiple renditions to capture the variation in the number of motifs, introductory notes, tempo, and syllable structure that are present in a male's repertoire. Thus, the five to seven examples we selected together captured the mean and range of bout compositions, including short, long, and average bout lengths and examples of the most common syntax as well as variants of the prototypical syntax. All selected song bouts were free of noise artifacts (e.g., cage noise) and we cropped songs to exclude call notes that preceded introductory notes or followed song termination. All song bouts were then band-pass-filtered (0.3-8.0 kHz), smoothed (Hanning window), normalized by the maximum amplitude and saved as wav files (44.1 kHz). We added two milliseconds of silence to the beginning and end of the song bouts after which we cosine ramped them to avoid sharp onsets and offsets in amplitude.

Stimuli used in the fMRI ON-OFF block paradigm had particular requirements, and we generated additional, fMRI specific stimulus sets for three different males. Each set consisted of four stimulus types: unmanipulated FD song, unmanipulated UD song, manipulated FD song (mFD) and a control song manipulation (mCTRL; Figure 6A). For each stimulus type, we generated five to seven different examples. The presentation of stimuli for fMRI in an ON-OFF block paradigm required that all stimuli be 16 s long with minimal silence between motifs. To achieve this, we concatenated together multiple song bouts from a single male to create each 16 s-long stimulus.

The manipulated stimuli switched the temporal and spectral characteristics between the FD and UD songs. Specifically, for one type (mFD), UD song syllables (spectral characteristics) were presented with the temporal characteristics (intersyllable and intermotif intervals) of FD song. To generate the manipulated stimuli, we determined syllable boundaries for all syllables in all of the recordings that we had for each bird using an automated, amplitude-based segmentation algorithm in MATLAB. Each syllable was then given an identifying label and we measured the duration of all syllables and gaps in the FD and UD songs that we recorded from a single male. We also measured the specific durations of syllables and gaps in each of the concatenated FD and UD stimuli described above. To create the mFD stimuli, we replaced each syllable in each concatenated FD song with a UD syllable of the same syllable type. We selected UD syllables with durations that exactly matched the durations of the specific syllable in the concatenated FD song they replaced. For the inter-syllable intervals, we used the measurements of the inter-syllable intervals in the concatenated stimuli to create silent gaps between syllables. Thus, the manipulated stimuli replicate the syllable and interval durations of each concatenated stimulus. To control for subtle effects resulting from the cutting and pasting of syllables, including increased amplitude contrast at syllable onsets and offsets, we created modified control stimuli (mCTRL) that contained FD song syllables. For the mCTRL we selected FD syllables with durations that exactly matched the durations of the specific syllables in the concatenated FD song that they replaced. None of the syllable renditions appear more than once in the stimulus sets. All manipulations were performed using custom written MATLAB routines. The same FD, UD, mFD and mCTRL stimuli that were used for the fMRI stimuli were also used for the behavior tests.

For the fMRI experiment, we also created additional artificial stimuli (16 s) consisting of pure tones at different frequencies between 1 and 7 kHz with durations of 0.7 s interleaved with silence periods of 0.1 to 0.2 s. The artificial frequency dependent increase of

sound intensity by the scanning setup was controlled by applying an equalizer to the stimuli upon presentation in the fMRI experiment [16]. Behavioral experiments were performed using the stimuli generated for the fMRI ON-OFF block paradigm.

For the fMRI experiment, we also created additional artificial stimuli (16 s) consisting of pure tones at different frequencies between 1 and 7 kHz with durations of 0.7 s interleaved with silence periods of 0.1 to 0.2 s. The artificial frequency dependent increase of sound intensity by the scanning setup was controlled by applying an equalizer to the stimuli upon presentation in the fMRI experiment [16]. Behavioral experiments were performed using the stimuli generated for the fMRI ON-OFF block paradigm.

Functional MRI

Data acquisition

We imaged 19 adult females on a horizontal MR system (Pharmascan 70/16 US, Bruker Biospin, Germany) with a magnetic field strength of 7 Tesla following established protocols [16]. More specifically, first, the birds were anaesthetized with isoflurane (IsoFlo, Abbott, Illinois, USA; induction: 3.0%; maintenance: 1.2%) in a mixture of oxygen and nitrogen (at flow rates of 100 and 200 cm^3/min, respectively) delivered through a beak mask fixed to the MRI scanner bed. Second, we acquired Turbo RARE T_2-weighted pilot scans along three orthogonal directions to inform on the birds' position in the MRI scanner. Based on these scans, we made sure all birds were positioned similarly (relative to the center of the scanner) for all imaging sessions. Third, we acquired two time series of 298 T_2-weighted rapid acquisition relaxation-enhanced (RARE) volumes for each bird with the following parameters: TE_{eff}/TR: 60/200 ms; matrix: 64x32 zerofilled to 64x64; slice number: 15; spatial resolution: (0.25x0.50x0.75)mm^3 zero-filled to (0.25x0.25x0.75)mm^3; interslice gap: 0.05 mm; FOV: (16x16x12)mm^3 (encapsulating the entire brain); orientation: sagittal; RARE factor: 8; scan duration: 40 min. In between the two fMRI time series, we obtained a 3-dimensional T2-weighted anatomical RARE scan with the following settings: TE 11 ms (TE_{eff} 44 ms), TR 3000 ms, RARE factor 8, FOV (16 × 14 × 14) mm^3, matrix (256 × 92 × 64), spatial resolution (0.06 × 0.15 × 0.22) mm^3 zerofilled to (0.06 × 0.05 × 0.05) mm^3, scan duration 35 min. The 3-dimensional T2-weighted RARE scan was acquired in the same orientation as the fMRI scans to facilitate later spatial registration of the fMRI.

Auditory stimulation was delivered at 70dB through dynamic loudspeakers (Visation, Germany; magnets removed), placed at each side of the bird's head. We presented females with one of four stimulus sets over two testing sessions, with one session for non-manipulated (FD song, UD song) stimuli and one for manipulated (mFD, mCTRL) stimuli. Besides these biologically relevant or modified sounds, we included a set of reference stimuli in the form of pure tones in each session to enable comparison of stimuli across sessions (e.g., FD/PT versus mDF/PT). We presented the three different stimulus types randomly in each session in an ON/OFF blocked design where 16 s of stimulation (ON periods) and 16 s of rest (OFF period) were alternated. The presentation order of the three stimulus types during the fMRI acquisition was randomized. In addition, for the FD and UD song stimuli the presentation of the different renditions of song was randomized over the stimulation blocks for the particular stimulus type. A session consisted of 72 ON blocks (24 per stimulus type) and 72 OFF blocks. During each block, we acquired two fMRI scans resulting in 48 time-series per stimulus type and per subject. The two fMRI sessions were separated by 40 min (during which the 3-dimensional T2-weighted RARE scan was acquired) and the order of manipulated and unmanipulated stimulus sets was randomized across birds.

Throughout the entire imaging protocol, the physiological condition of the animals was continuously monitored by means of a pressure sensitive pad to detect the breathing rate, and a cloacal thermistor probe to measure body temperature (MR-compatible Small Animal Monitoring and Gating system, SA Instruments). The latter was connected to a tightly controlled warm air feedback system to maintain the birds' body temperature within narrow physiological ranges (40.0 ± 0.2)°C. All zebra finches recovered uneventfully within a few minutes after the experiment.

Data quality assessment

We applied the following inclusion criteria for the fMRI time series: (1) limited head motion (< 0.5 mm translation in either of 3 directions), and (2) detection of positive BOLD response in the primary auditory region Field L. In the event that one of these criteria was not met, we repeated the fMRI experiment for that particular individual using stimuli from a different male to ensure unfamiliarity of the presented sounds during scanning. Doing so, a final success rate of more than 80% was reached, which is in line with previous fMRI experiments in zebra finches [21, 61, 62].

Data processing

We performed both data preprocessing and voxel-based analysis using the Statistical Parametric Mapping toolbox (SPM12, Wellcome Trust Centre for Neuroimaging, London, UK; http://www.fil.ion.ucl.ac.uk/spm) as described in [16] with some adaptations. First, we realigned each fMRI scan time series (correct for translation and rotation of the bird's head during scanning) and co-registered them to their corresponding 3D RARE acquired during the same imaging session using mutual information as similarity metric. Second, we masked the 3D RARE scan to exclude non-brain tissue. This step appeared necessary to facilitate subsequent spatial normalization steps. Third, we spatially normalized all 3D RARE images to the high-resolution zebra finch MRI atlas [22] using a global 12-parameter affine transformation followed by nonlinear deformations. The spatial correspondence between each individual scan and the *ex vivo* zebra finch MRI atlas was inspected visually. In case the spatial transformation did not reach satisfactory standards, the procedure was repeated until successful. Fourth, we up-sampled the fMRI data to a final resolution of (0.125 × 0.125 × 0.400) mm^3 [63] and applied the spatial transformation parameters estimated during the previous step to the co-registered fMRI scan time series. This way all fMRI data were transformed into the zebra finch MRI atlas space. Fifth, we smoothed the fMRI images in-plane using a Gaussian kernel of 0.5 mm full width at half maximum (FWHM).

We applied a high pass filter (352 s cutoff period) to the data to remove low-frequency drifts in the BOLD signal. For each subject, we subsequently modeled the BOLD responses as a box-car function convolved with a canonical hemodynamic response function within the framework of the general linear model to analyze brain activation differences related to the onset of the different stimuli. We included the six estimated movement parameters derived from the realignment corrections as regressors in the model to account for the residual effect of head motion. After the estimation of the GLM parameters (β), we calculated different t-contrast images (containing weighted parameter estimates) for different comparisons including FD song, UD song, mFD and mCTRL > rest and > pure tones. These single subject contrast maps were subsequently entered into appropriate statistical designs for group analysis.

The clusters in which a significant selectivity for FD song was found in the voxel-based group analysis (see Results) were used as regions of interest (ROIs) in the subsequent ROI based analysis. To compare responses in the left and right hemisphere, the ROIs identified in one hemisphere were mirrored over the midline to obtain an identical ROI in the opposite hemisphere. From the single subject t-contrast maps for FD song > rest and UD song > rest, we subsequently calculated the average fMRI signal over the contiguous voxels in each ROI.

EGR1 expression

Adult females (n = 24) that had not been exposed to fMRI imaging or behavior tests were placed individually in sound-attenuating chambers for at least 24 hr prior to experimentation. The morning of the experiment, we turned lights off at least 2 hr before initiating 30 min of song playback of either FD or UD song from a single male through a speaker (Avantone, New York). We played back five to seven FD or UD stimuli from a single male at 70 dB in random order with each stimulus separated by one second. As with scanning during fMRI, we performed playback in the dark to minimize female calling and ensure responses were only to auditory cues that occurred during the stimulation period. Females who were not exposed to song playback but were otherwise treated identically to birds receiving playback, were used as silence controls. After song playback, we kept females in the dark, undisturbed, for 45 min to allow for protein translation [13, 64]. Subjects were then deeply anaesthetized with isoflurane vapor and transcardially perfused with 25 mL heparinized saline (100 IU/100mL) followed by 150 mL of 4% paraformaldehyde (pH 7.4). Brains were collected and post-fixed for 4 hr, then cryoprotected in 30% sucrose. We cut 40 μm sagittal sections from the left and right hemispheres on a freezing microtome (Leica Biosystems, Wetzlar, Germany) and stored these in 0.025M phosphate-buffered saline (PBS) with sodium azide at 4°C.

For the analysis of the expression of EGR1, we performed ICC in ten batches, each of which contained every third section from one bird that heard FD song and one that heard UD song. Both song-exposed birds in the batch heard songs from the same stimulus male. Four batches also included a silence control. We followed standard ICC procedures that have been described elsewhere [14, 56, 65–67]. Briefly, brain sections were rinsed (3 X 10-min) in 0.025M PBS then incubated in 5% donkey serum and 0.3% Triton-X. Following additional rinses (3X10 min) sections were incubated for 48-h at 4°C in rabbit anti-EGR1 (1:1000 dilution; Santa Cruz Biotechnology, Santa Cruz, CA, USA) and either sheep anti-tyrosine hydroxylase (TH; n = 7 batches; 1:1000 dilution; Cat# NB300-110, Novus Biologicals, Littleton, CO, USA) or mouse anti-NeuN (n = 3 batches; 'Neuronal Nuclei'; 1: 1000 dilution; Cat# MAB377; EMD Millipore, Billerica, MA, USA). Sections were then washed (3 X 10-min) and incubated for 2-h at room temperature in donkey anti-rabbit secondary antibody conjugated to Alexa Fluor 594 (for EGR1; 5 μl/ml; Life Sciences, Burlington, ON, Canada) and either donkey anti-sheep (for TH) or donkey anti-mouse (for NeuN) secondary antibody conjugated Alexa Fluor 488 (3 μl/ml; Life Sciences). Following another wash (3 X 10-min), sections were mounted and coverslipped (ProLong Gold Antifade Reagent, Life Sciences) on chromium-aluminum subbed slides.

We imaged EGR1-immunoreactive (EGR1-ir) neurons in the two regions found to be selective for FD song in the fMRI experiment, the CMM and the NCC. For the CMM, we sampled in the most caudal area dorsal to the mesopallial lamina and ventral to the lateral ventricle [13]. The results for this region served as a control group in a previously published study [14]. For the identified region in the NC, sampling was guided by the MRI results. Lateral sections from batch 1-3 were not available, so NC analysis was only performed in batches 4-10. Damaged sections were excluded and if fewer than two sections remained for a given hemisphere of a specific region, the result for that hemisphere was left out of the statistical analysis (n = 1 (UD) for right CMM; n = 1 (FD) for left NCC; n = 1 for right NCC). For each region, monochrome photomicrographs of EGR1 expression were taken in each hemisphere with a 40X objective using a Zeiss Axio Imager upright microscope and an AxioCam MRm Zeiss camera (Carl Zeiss, Jena, Germany). Using Fiji imaging software (NIH), EGR1-ir neurons were manually counted in a (225 X 170) μm^2 window on multiple sections (see Figure S2 for representative images). Imaging and cell counts were performed by a researcher blind to the playback condition of the individual bird. Fiji was used to ensure consistency of thresholds for determining labeled neurons across sections within an individual bird as well as between birds.

TH expression

Two females and two males were deeply anaesthetized with sodium pentobarbital (Doléthal, 0.25 g/kg, i.p.) and transcardially perfused with ice-cold saline (pH 7.4) followed by 4% paraformaldehyde (pH 7.4). Brains were collected and post-fixed overnight (< 15 hr) then cryoprotected in 20% sucrose (4°C, 10 hr) followed by 30% sucrose. We cut 40 μm coronal sections in 10 parallel series (Leica Microsystems, Wetzlar, Germany) and stored these in 0.1% sodium azide in PBS at 4°C. As previously described [68], the immunochemical detection of TH took place in one series of free-floating sections with the avidin/biotin-technique visualized by 3,3′-diaminobenzidine (DAB) with cobalt-nickel enhancement [69]. The protocol was refined with the addition of a defixation step using heat-induced-epitope-retrieval [70], and an optimal antibody concentration as established in different avian species (von Eugen,

unpublished). More specifically, the protocol consisted of the following steps which were all performed at room temperature, unless otherwise stated. Incubation was done using a slow 7° rotator and washes (3 X 10 min) in 0.12 M PBS were done on a slow 5° rotator. After an initial washing step of the slices, we performed heat-induced epitope-retrieval. One series of free-floating sections were placed in 10 mM preheated sodium citrate (pH 8.5-9.0) and maintained at 80°C for 30 min. The slides were then washed and incubated in 0.6% H_2O_2 in 0.12 M PBS to deactivate endogenous peroxidase. After another washing step, sections were incubated for 30 min in 10% normal-horse-serum (NHS) in 0.3% Triton X-100 in 0.12 M PBS (PBST). Next, slides were washed and incubated in the primary antibody (monoclonal mouse anti-TH (MAB5280, MerckMillipore, Darmstadt, Germany), 1:500 in PBST) for 70 hr at 4°C. Following incubation, slides were washed again and incubated in the secondary antibody (biotinylated horse anti-mouse IgG (Vectastain Elite ABC Kit, Horse IgG, Vector), 1:500 in PBST) for 1 hr. After another washing step, sections were incubated in avidin/biotin complex (Vectastain Elite ABD Kit, 1:100 in PBST) for 1 hr. The bound complex was visualized with 3,3′-diaminobenzidine (DAB; Sigma-Aldrich) with cobalt-nickel enhancement. After staining, sections were mounted on gelatin-covered glass slides, dried, dehydrated, and coverslipped using DePex (Sigma-Aldrich). Subsequently, we selected the left and right hemisphere of the eight most caudal slices based on previous descriptions of TH distribution in the zebra finch [71] and on the location of the NC sub-region from the fMRI analysis (see fMRI results). Pictures were taken using a Zeiss Axio Imager M1 Microscope (Carl Zeiss MicroImaging, Gottingen, Germany) with the 20x objective as well as a 40x objective within regions of interest for a closer examination of basket morphology.

We assessed TH fiber density using a custom written automatic program (Sepideh Tabrik, research assistant at Ruhr-Universität Bochum, Germany). Following [72], the program employs a Hessian based curvilinear feature extraction in ImageJ (version 1.48, U.S. National Institutes of Health, Bethesda, Maryland, USA). Hessian image filters are most suitable to extract curvilinear structures, and thus fibers. Next, we executed a baseline adjustment and peak detection on the filtered images in MATLAB (version R2016a, MathWorks, Natwick, MA, USA). The baseline adjustment increases the signal to noise ratio within the image, and the peak detection quantifies the number of high-intensity pixels above a specified threshold, representing the stained fibers, on a projected (grid)-line. The threshold was determined from an unstained area within the brain slide. The program returns an approximation of TH^+-fiber density per 150 μm^2 over the whole brain slice. These results allowed for a qualitative analysis of the trajectory of fiber density differences throughout the caudal telencephalon of two females, which we verified with data from two males.

Call-back behavior

We assessed female responses to FD and UD songs using a call-back assay [73, 74]. At least 24h prior to testing, females were moved into a sound-attenuating chamber equipped with a microphone, a video camera and a speaker. We performed the assays between 9am and 2pm over the course of one day. The call-back assay for each stimulus consisted of a 15-minute silent period ('pre-stimulus period') followed by 5 min of stimulus playback and then another 10-minute period of silence ('stimulus period'). For each five-minute block of song playback, multiple renditions of FD and UD song from a single male were played through a speaker in pseudorandom order using custom written MATLAB routines. A one-second interval was included between each rendition resulting in a total duration of song played within the stimulus period of 4.19 ± 0.01 min. Thirteen females were tested with FD and UD songs from a single stimulus male as well as modified versions of the song (mFD and mCTRL). The order of stimulus presentation was randomized for each female. Sound was recorded continuously throughout the entire period of testing using SAP.

The number of calls in the pre-stimulus and stimulus period were counted manually, by a person blind to the experimental conditions, using custom written MATLAB routines. No distinction was made between call types. To assess females' responses to the different song types, we calculated the percent change in call-back behavior in response to the stimulus playback (% call-back):

$$\%\ call-back = \frac{calls_{stimulus} - calls_{pre-stimulus}}{calls_{stimulus} + calls_{pre-stimulus}}$$

A positive value for the % call-back indicates thus an increase in calling after presentation of the song as compared to the pre-stimulus period, whereas a negative value indicates a decrease in calling.

QUANTIFICATION AND STATISTICAL ANALYSIS

fMRI group analysis

Statistical voxel-based group analysis of the fMRI data was done in SPM12 (Wellcome Trust Centre for Neuroimaging, London, UK; http://www.fil.ion.ucl.ac.uk/spm). The Family Wise Error (FWE) method was applied to adjust p values to the number of independent tests performed. This method uses the Random Field Theory to calculate the number of independent tests, taking into account the number of voxels as well as the amount of auto-correlation among the data. Data were considered significant for $p_{FWE}<0.05$ with a minimal cluster size of 5 voxels. For whole brain analyses, FWE correction appeared too conservative to detect any effects, therefore, in such analyses a statistical threshold of $p < 0.001$ without any correction for multiple comparisons (p_{uncorr}) was applied with a minimal cluster size of 10 voxels but without any correction for multiple comparisons (p_{uncorr}). Reflecting the voxel basis of the analysis, results are reported by the highest voxel T value within each cluster (T_{max}) and the associated voxel p value.

In a first stage of the group analysis, we considered only the response to FD and UD song in order to determine the selective neural substrates of FD song perception at the level of the whole brain. For this, we entered the single subject t-contrast images

for FD song > rest and UD song > rest into a paired t test design for FD > UD song. Subsequently, we converted these FD song selective clusters (using a significance level of $p_{uncorr}<0.001$) into regions of interest (ROIs) for further in depth analysis.

In a second stage, we considered data from both fMRI sessions to determine differential responses to mFD or mCTRL versus FD and UD song stimulation within these ROIs. As these data originated from two separate fMRI time series as described above, we used the single subject t-contrast images with the pure tones as reference (used as identical reference stimulus in both sessions) in this analysis. Before including the pure tones as a reference in the analysis, we verified responses to this stimulus at the whole brain level by entering the single subject t-contrast images for pure tones > rest into a one sample t test (see Figure S1A). For statistical analysis of the differences in response to mFD or mCTRL versus FD and UD song, we entered the individual single subject t-contrast images into a flexible factorial design with subjects as random variable. We explored the main effect of stimulus and performed individual t tests to investigate the origin of the differences in the responses to the different stimuli. A statistical threshold of $p_{FWE}<0.05$ was applied with correction at the level of the respective ROIs.

Besides voxel based group analysis, we also performed an ROI analysis to compare average responses between FD and UD song over hemispheres. For this, we performed a repeated-measures ANOVA analysis with stimulus and hemisphere as within-subject factors using IBM SPSS Statistics for Windows (Version 22.0. Armonk, NY: IBM). Bonferroni correction was applied for all post hoc tests with $\alpha < 0.05$.

Finally, we also analyzed the responses to pure tones within both ROIs. Specifically, for the NCC and CMM, we used two mixed-effects models, one to test for differences between the stimuli and a second to test for differences between the hemispheres. In both cases, BOLD response was the dependent variable and bird ID was included as a random variable. We used Tukey's HSD (honest significant difference) test for all post hoc tests with $\alpha < 0.05$ unless otherwise noted.

EGR1 expression analysis

We analyzed whether stimulus context (FD versus UD song) influenced EGR1 expression in the CMM and the NCC. We first checked for the normality of the raw data and the residuals by looking at the linearity of quantile-quantile plots and fitting a normal curve to the distribution followed by a Shapiro-Wilk W test of the goodness of fit of the curves. If data or residuals were non-normally distributed, we performed data transformations to improve normality. Here, we report the results for log transformed data, although box-cox transformations were similarly effective. We then used a mixed-effects model with stimulus context (FD versus UD song), hemisphere (left versus right), and the interaction as the independent variables and batch and bird ID nested within batch as random variables. We analyzed the number of EGR1-ir cells/mm^2, or the log number of EGR1-ir cells/mm^2, as the dependent variable. Unbounded variance components were used and the restricted maximum likelihood method was applied to fit the data. We found no significant interaction between stimulus context and hemisphere in any of the brain regions and thus report only the results for the main effects of stimulus context and hemisphere. Silent controls were not included in the statistical analyses but are presented in the figures to allow visual comparison. We performed the statistical analysis in JMP® (Version 13, SAS Institute, Cary, NC, 1989-2007) and used Tukey's HSD (honest significant difference) test for all post hoc tests with $\alpha < 0.05$ unless otherwise noted.

Call-back analysis

We investigated the differences in call-back to the different stimuli using a mixed-effects model with unbounded variance components and the restricted maximum likelihood method to fit the data. % call-back was analyzed as the dependent variable while female ID was included as a random variable. The analysis was performed in JMP® (Version 13, SAS Institute, Cary, NC, 1989-2007) and we used Tukey's HSD test for all post hoc tests with $\alpha < 0.05$ unless otherwise noted.

We also analyzed variation in the ranking of the four stimuli. In particular, we noted that while most females exhibited the greatest increases in calling to FD song, the responses to the other three stimuli were generally both lower and more variable. To analyze these differences, we ranked the responses of each bird to the four stimuli, with 1 indicating the most positive response and 4 as the most negative response. In the event of at tie, more than one stimulus could receive the same ranking. We then performed a contingency analysis with stimulus type as the independent variable, ranking as the ordinal dependent variable, and bird ID as a third classification variable to account for repeated-measures. We used the Cochran Mantel Haenszel χ^2 tests to compare all pairs of stimuli to test for linear relationships between stimulus and ranking across bird IDs.

DATA AND SOFTWARE AVAILABILITY

All data are available upon request to the authors.